

## Effect of small-scale baryon inhomogeneity on cosmic nucleosynthesis

Hannu Kurki-Suonio

*Department of Physics, Drexel University, Philadelphia, Pennsylvania 19104*

Richard A. Matzner

*Center for Relativity and Department of Physics, University of Texas at Austin, Austin, Texas 78712-1081*

(Received 13 September 1988)

We consider the evolution of the nuclear abundances in a universe with inhomogeneities (induced by the quark-hadron phase transition) on a scale such that neutron diffusion is important before and during nucleosynthesis. We investigate a number of initial baryon density contrast ratios:  $R=10, 100, 1000$ ; a number of high-density volume fractions:  $f_V = \frac{1}{4}, \frac{1}{8}, \frac{1}{16},$  and  $\frac{1}{64}$ ; and a number of geometries: planar, cylindrical with the higher density near the center, cylindrical with the higher density near the outer zone of computation (thin-walled tubes of higher density), spherical with the higher density near the center (isolated spherical regions of high density), and spherical with the higher density near the outer zones of the computation (a foam structure of high-density regions). We concentrate on three  $R=100$  models. For a high-density [ $\eta=70 \times 10^{-10} \equiv \rho_{\text{baryon}}(\text{now}) = 4.3 \times 10^{-30} \text{ g cm}^{-3}$ ] universe that would be closed for Hubble parameter  $H_0=50 \text{ km/sec Mpc}$ , we find disagreement in all three isotopes ( $^2\text{H}, ^4\text{He}, ^7\text{Li}$ ) with observations, regardless of the scale  $r_i$  of the inhomogeneity; for  $\eta=3 \times 10^{-10}$  and  $\eta=7 \times 10^{-10}$ , "low"- and "high"-standard values ( $\eta=3 \times 10^{-10}$  corresponds in the homogeneous case to the absolute minimum of  $^7\text{Li}$  production), we find that for inhomogeneity distance scales typical of those expected at the quark-hadron transition, i.e.,  $r_i \lesssim 100 \text{ m}$ , then  $^4\text{He}$  and  $^2\text{H}$  abundances remain in agreement with observational values, and  $^7\text{Li}$  is also not much changed from its value in a homogeneous cosmology.

### I. INTRODUCTION

Recently there has been considerable interest in the possibility that the quark-hadron phase transition (at  $T \gtrsim 100 \text{ MeV}$ ) could have affected the cosmic nucleosynthesis (at  $T \lesssim 100 \text{ keV}$ ) through the generation of a small-scale inhomogeneity in the baryon-number density.<sup>1-12</sup>

The relative abundances of the light elements produced in the early Universe depend on the baryon-to-photon ratio  $n_b/n_\gamma$ . This dependence has been used to determine the density of baryonic matter in the Universe, assuming that the Universe was homogeneous and isotropic when the nucleosynthesis took place;<sup>13,14</sup> see Fig. 1.

What if the Universe were inhomogeneous? We address here the question of inhomogeneity in the baryon density alone and assume a homogeneous background. Because the early Universe was radiation dominated, the baryon density was dynamically insignificant, and any initial inhomogeneity would have just retained its shape until eventually smoothing out by diffusion. If the distance scale of the inhomogeneities is significantly larger than the diffusion distance—as had usually been assumed in the past, since the diffusion distance at the time of nucleosynthesis was several orders of magnitude smaller than the horizon distance—one then gets what we refer to as the effect of  $n_b/n_\gamma$  inhomogeneity. In this case the produced average light-element abundances can be obtained simply by calculating the properly weighted averages from homogeneous nucleosynthesis results with

different densities. The  $n_b/n_\gamma$  inhomogeneity in most cases raises the  $^4\text{He}, ^2\text{H},$  and  $^7\text{Li}$  abundances. The results are independent of the inhomogeneity distance scale as long as it is large enough that diffusion can be ignored.

As first noted by Applegate, Hogan, and Scherrer<sup>2,3</sup> (AHS), things change when there is significant diffusion. Of course, if the distance scale is small enough to allow diffusion to completely eliminate the inhomogeneity, we return to the homogeneous case. There is, however, an *intermediate* distance scale where diffusion has a very interesting effect on nucleosynthesis. The reason for this is that as we approach nucleosynthesis, neutrons will be diffusing several orders of magnitude faster than protons. Thus, diffusion will create an *n/p inhomogeneity* in addition to the  $n_b/n_\gamma$  inhomogeneity.

The distance scales where diffusion begins to have an effect are so small that the baryon number in one "lump" is smaller than that of a small star. Thus, only averaged final abundances are of interest here.

When it was predicted that the quark-hadron phase transition would create a baryon inhomogeneity with a distance scale within this interesting range, it became important to study its effect on nucleosynthesis. The first studies<sup>3,4</sup> used a simplified model where the neutrons were assumed to diffuse completely to an homogeneous neutron density before nucleosynthesis, and then all diffusion effects during nucleosynthesis were ignored. We refer to this as the *simple-diffusion* model. This kind of nucleosynthesis with a neutron-rich low-density region and a proton-rich high-density region led to a significant

reduction in the total  ${}^4\text{He}$  production and an increased  ${}^2\text{H}$  production (beyond the  $n_b/n_\gamma$ -inhomogeneity effect), making it easy to satisfy both  ${}^4\text{He}$  and  ${}^2\text{H}$  constraints with a critical baryon density ( $\Omega_b=1$ ), with a density contrast ( $\geq 50$ ) that did not seem inconceivable from the quark-hadron transition. This was very attractive because if the baryon density is this high, we would not need to postulate exotic new particles to account for the "missing mass" of the Universe.

${}^7\text{Li}$  seemed to be overproduced in those calculations, however, mainly because of the  $n_b/n_\gamma$  effect. To solve this problem, it was proposed that  ${}^7\text{Li}$  (or actually the  ${}^7\text{Be}$ , which would later  $e^-$  capture to  ${}^7\text{Li}$ ) would be destroyed by neutrons diffusing back to the high-density regions after nucleosynthesis.<sup>11</sup> On the other hand, since inhomogeneity seemed to lead to a significant increase in  ${}^7\text{Li}$  production, even with a "standard" average

$n_b/n_\gamma \sim (3-7) \times 10^{-10}$ , it was claimed that the  ${}^7\text{Li}$  constraint actually rules out any strong baryon inhomogeneity at nucleosynthesis time.<sup>15</sup>

The preceding model was, however, oversimplified. If diffusion is important before nucleosynthesis, it is also important during nucleosynthesis (unless even the  $p$  inhomogeneity has been erased by that time). The intermediate distance scale is thus the most difficult to study, necessitating the use of an inhomogeneous nucleosynthesis code with a large number of zones, where nucleosynthesis within each zone is computed simultaneously with zone-to-zone diffusion. Using such a code, we found that most of the neutron-diffusion effect on the  ${}^4\text{He}$  and  ${}^2\text{H}$  abundances seen in the simplified model was erased.<sup>10</sup> The reason is that nucleosynthesis begins first in the high-density regions, and the neutrons in the low-density regions then diffuse back into the high-density regions. The strongest effects from neutron diffusion were obtained in a narrow distance range, where the distance is so long that diffusion only partly smooths the  $n$  distribution, and then only part of the neutrons will diffuse back into the high-density region. These results<sup>10</sup> were obtained using a plane-symmetric cosmology code, which was originally written with very different situations in mind.<sup>16-19</sup> Thus the code was rather expensive to run in the small-scale diffusion situation, and we had to limit ourselves to a very small number of runs. Also the results were all for a plane-symmetric inhomogeneity. It was questioned whether this is an appropriate geometry for the problem and whether the results might be very different for spherical high density regions.

Therefore, we wrote another code, specifically aimed at this problem, which allowed us to do a much larger number of runs, with different geometries, and to better cover the parameter space. We present our results here.

The task would be much simpler if we had a clear prediction of the scale, shape, and strength of the inhomogeneity resulting from the quark-hadron phase transition. Unfortunately the physics of the transition is too poorly understood for that. Thus we need a very large number of runs, with different inhomogeneities, to get an idea of the possible effects of such an inhomogeneity.

We have another reason not to tie our nucleosynthesis work too closely to the quark-hadron phase transition. Although it now seems quite plausible that there is considerable baryon-density contrast across the phase interface during the phase transition,<sup>20,21</sup> it is questionable whether this leads to a massive baryon inhomogeneity after the transition. This depends on unknown details, such as diffusion of baryon number in the quark-gluon plasma. We have discussed this earlier<sup>7</sup> and remain skeptical of the creation of a massive baryon inhomogeneity.

With our inhomogeneous code there is no need to stick to a simple two-density idealization of inhomogeneity. We decided, however, to do so due to absence of knowledge of the actual profile of the presumed inhomogeneities and since it facilitates comparison with earlier studies.<sup>3-6,9-12</sup> This kind of sharp division to high- and low-density regions brings out the effects of diffusion the most clearly.

The results will be used in two ways. First, we will see

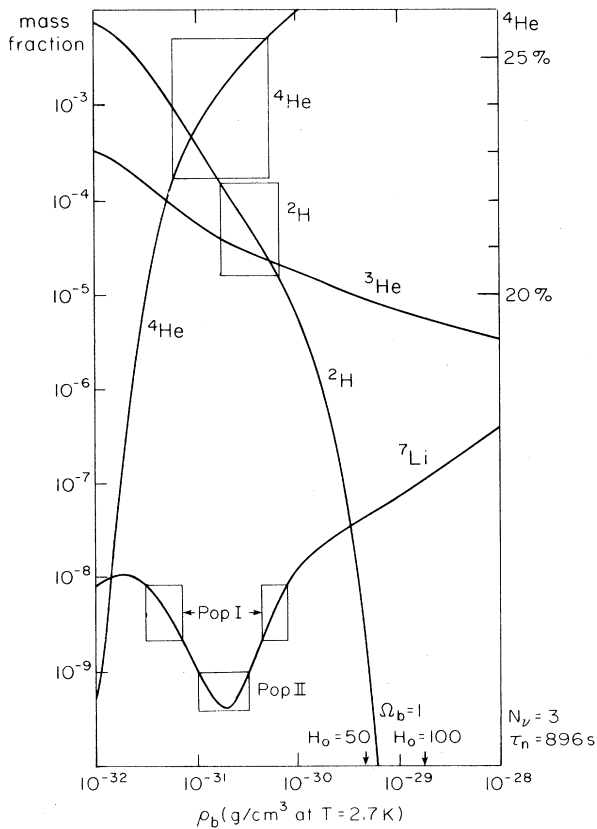


FIG. 1. Standard homogeneous nucleosynthesis results. We plot the primordial abundances calculated with our code in a homogeneous case as a function of the baryon density. The rectangles show the estimated primordial abundances based on astronomical observations (Ref 14). For  ${}^7\text{Li}$  there are two disjoint ranges, based on population I and population II stars. A simultaneous agreement for all the isotopes can be obtained between  $p_b = 10^{-31} \text{ g/cm}^3$  ( $\eta = 1.5 \times 10^{-10}$ ) and  $p_b = 10^{-30} \text{ g/cm}^3$  ( $\eta = 15 \times 10^{-10}$ ). This estimate for the present baryon mass density is at least 1 order of magnitude below the critical value ( $\Omega_b = 1$ ) required to recollapse the Universe.

whether the standard nucleosynthesis conclusions change if baryon inhomogeneity were present during nucleosynthesis. Second, we will use the results to put limits on the early baryon inhomogeneity. There are two specific questions we try to answer here. (1) Is it possible to satisfy the observational constraints on  ${}^2\text{H}$ ,  ${}^4\text{He}$ , and  ${}^7\text{Li}$  with a critical baryon density? (2) Do the observational constraints (especially  ${}^7\text{Li}$ ) rule out a strong baryon inhomogeneity at nucleosynthesis time, thereby perhaps placing constraints on the quark-hadron phase transition?

## II. THE COMPUTATIONAL MODEL

Our new inhomogeneous nucleosynthesis and diffusion code assumes an expanding homogeneous background, Friedmann-Robertson-Walker (FRW (0)) spacetime. We originally prepared for three-dimensional (3D) computations also, but it became obvious that because of the dense grid required for accurate results, we would not be able to do many 3D runs with presently available computer resources. The code has been tested only for the 1D case, and all the results presented here are from 1D runs. Within the 1D case, we can handle three different geometries: planar, cylindrical, and spherical. The geometry appears only in the treatment of the diffusion equation and in calculating averages. Our computational grid is divided into at least 64 evenly spaced zones. We use reflective boundary conditions (this doubles the accuracy or halves the number of zones needed, when compared to the periodic boundary conditions of the previous code<sup>10</sup>).

We start the computation at a temperature  $T_9 \equiv (T/10^9 \text{ K}) = 50$ , where we set the initial values of baryon density. Some zones are given a high density and others a low density. All our runs have been with this kind of two-density initial distribution. This obviously is a simplification; it should make the results easier to interpret and to compare with the work of others. In the cylindrical and spherical geometry, we have put the high-density region either at the center or at the boundary; thus we have studied five different shapes for the high/low-density regions.

The computation proceeds through time steps, where in each time step we first do an expansion step, then a diffusion step, and finally a nucleosynthesis step. The expansion step evolves the FRW (0) spacetime, changing the average baryon density with expansion and giving the distance scale for the diffusion step. We assume three flavors of massless neutrons.

The diffusion step is further divided into a neutron diffusion step and a proton diffusion step. Thus our code diffused both neutrons and protons but not the other nuclei. For the diffusion coefficients we use the values calculated by AHS, except that we have corrected their numerical value for  $D_{ne}$ , where the factor  $\pi/16$  was missing. Thus,

$$D_{ne} = 3.95 \times 10^9 \frac{e^{1/x}}{xf(x)} \text{ cm}^2/\text{s},$$

where  $x = T/m_e$  and  $f(x) = 1 + 3x + 3x^2$ . In the neutron diffusion coefficient we have included scattering from

electrons and positrons and from protons, but not from the other nuclei. This should not be a serious omission, since protons are much more abundant. If a region forms with a very high  ${}^4\text{He}$  fraction, our code overestimates the  $n$  diffusion through the region because the  ${}^4\text{He}$  nuclei are not "seen." The proton diffusion should not have a large effect in our runs because on the scales we are studying there is very little of it. We did a few runs both with and without proton diffusion to see how large an effect there is. We have ignored diffusion of other nuclei, which should have even less effect than that of protons.

The protons scatter from thermal electrons and positrons, which are still quite abundant at  $T_9 \simeq 1$ . Because proton scattering from neutrons and nuclei becomes important only after nucleosynthesis, we have not paid attention to it. To prevent numerical problems towards the end of the run, when electrons and protons have annihilated, the code has

$$D_p^{-1} = D_{pe}^{-1} + D_{np}^{-1};$$

i.e., protons are not allowed to diffuse faster than neutrons.

Our diffusion time step is fully implicit. The diffusion coefficient is inhomogeneous because it depends on the proton density. For each zone edge we use the average of the proton densities at the two neighboring zones before the diffusion step.

Because we compute the weak  $n \leftrightarrow p$  reactions in the nucleosynthesis time step, there is no need to introduce any cutoff temperature below which the neutrons and protons retain their identities and begin to diffuse at different rates, as was done in the simple-diffusion model.

The nucleosynthesis time step is done independently for each zone. Our reaction network contains all 30 strong reaction rates listed by Fowler, Caughlan, and Zimmermann<sup>22,23</sup> and Harris, Fowler, Caughlan and Zimmerman<sup>24</sup> that involve nuclei with mass numbers  $A \leq 7$  only, and their inverse reactions. Those are sufficient to calculate the cosmologically significant isotopes  ${}^2\text{H}$ ,  ${}^3\text{He}$ ,  ${}^4\text{He}$ , and  ${}^7\text{Li}$ . We use a neutron mean lifetime  $\tau_n = 896 \text{ s}$  (Ref. 25).

The code runs until the temperature has dropped to  $T_9 = 0.025$ , by which time the strong nuclear reactions have essentially ceased and the total amounts of the primordial isotopes are determined. The time step follows the expansion so that the relative expansion is the same in each time step, except that during the main nucleosynthesis action a shorter time step is used: For the temperature range  $T_9 = 0.25 - 1.0$ , the time step is reduced to  $\frac{1}{4}$  and during the main  ${}^4\text{He}$  production, the time step is made even shorter by tying it to the change in total  ${}^4\text{He}$  fraction so that about 25% of the code time is spent in the short period when most of the  ${}^4\text{He}$  is produced. A typical run thus uses about 6000 time steps from  $T_9 = 50$  to  $T_9 = 0.025$ .

The code was tested by checking that in the small-distance-scale limit in the results agree with the standard homogeneous nucleosynthesis results and that in the large-distance-scale limit the results agree with the weighted average of the homogeneous results for the high and low densities.

The accuracy of the results were confirmed by repeating the runs three times: with a doubled time step, with a doubled grid spacing, and with both a doubled time step and a doubled grid spacing. We required that the  ${}^4\text{He}$  fraction should not change by more than 0.001 and that the common logarithms of the other mass fractions should not change by more than 0.05. In some runs we had to go to 128 or 256 grid zones and to 12 000 or 24 000 time steps to achieve the required accuracy. The most difficult cases were the runs with the highest density contracts, the runs where a small high-density volume fraction made the number of high-density zones very small, and the runs with the intermediate distance scale, where the neutron-diffusion effects were strongest, expect that accurate deuterium values with  $\rho_b = \rho_{\text{crit}}$  were the most difficult to obtain with smaller distance scales where  ${}^2\text{H}$  was rapidly approaching (as a function of the distance scale) the low homogeneous nucleosynthesis values.

### III. RESULTS

With our simplified two-density form for the inhomogeneity, there still remain five parameters to specify the baryon inhomogeneity. They are  $\eta$ , the average baryon-to-photon ratio,  $R$ , the density contrast between the high- and low-density regions,  $f_v$ , the volume fraction of the high-density region,  $r_1$ , the distance scale of the inhomogeneity, and the geometry, i.e., the shape of the regions.

The baryon-to-photon ratio is related to the present baryon density through

$$\eta_{10} \equiv \eta / 10^{-10} = 15.0 \times \rho_b (2.7 \text{ K}) / 10^{-30} \text{ g cm}^{-3}.$$

The distance scale  $r_1$  is the length of our grid, which in our computations has only one high-density region. Because we use reflective boundary conditions,  $r_1$  corresponds to half the distance between the centers of neighboring high-density regions. The grid is comoving, i.e., "expands" with the Universe. Therefore, the distance scale is given in comoving units or has to be specified at a certain moment. We refer to it in units of present ( $T=2.7 \text{ K}$ ) light hours (h). This unit corresponds to about one meter at  $T=100 \text{ MeV}$  if the Universe is in the quark phase, and to about 1.5 m if in the hadronic phase. At  $T_9=1$ , when nucleosynthesis is about to begin, it corresponds to 2.5 km.

We did runs with three different values of average baryon density,  $\eta_{10}=3, 7$ , and 70. The highest value 70 corresponds to the critical density for  $H_0=50 \text{ km s}^{-1} \text{ Mpc}^{-1}$ . The values 3 and 7 are low and high "standard" values, respectively. In the standard homogeneous model,  $\eta_{10}=7$  gives  ${}^4\text{He}$  close to its upper observational limit and a low population I  ${}^7\text{Li}$  value.  $\eta_{10}=3$  corresponds to minimum  ${}^7\text{Li}$  production (a low population II value) and fairly high  ${}^2\text{H}$ .

For most of our runs, we used three values for the density contrast,  $R=10, 100$ , and 1000. We concentrate here on the  $R=100$  runs, since higher values seem implausible and lower values lead to less prominent effects. For the high-density volume fraction, we used values  $\frac{1}{4}, \frac{1}{8}, \frac{1}{16}$ , and  $\frac{1}{64}$ ; and for the distance scale  $r_1=1000, 500, 200, 100, 50, 20, 10, 5, 2$ , and 1 h.

We concentrate here on two geometries, planar and spherical, with high density at the center. The results from a spherical case with high density at the outermost zones were very similar to the planar case, except for a shift in distance scale, so that the same *thickness* of the high-density region tended to yield similar results, instead of the same  $r_1$ . The results from the cylindrical geometry were intermediate between the planar and the spherical geometry.

Our  $R=100$  results with the two geometries are shown in Figs. 2–4. We present the results as a function of the distance scale  $r_1$ . The results are very sensitive to  $r_1$ , since it determines the neutron diffusion effects. The

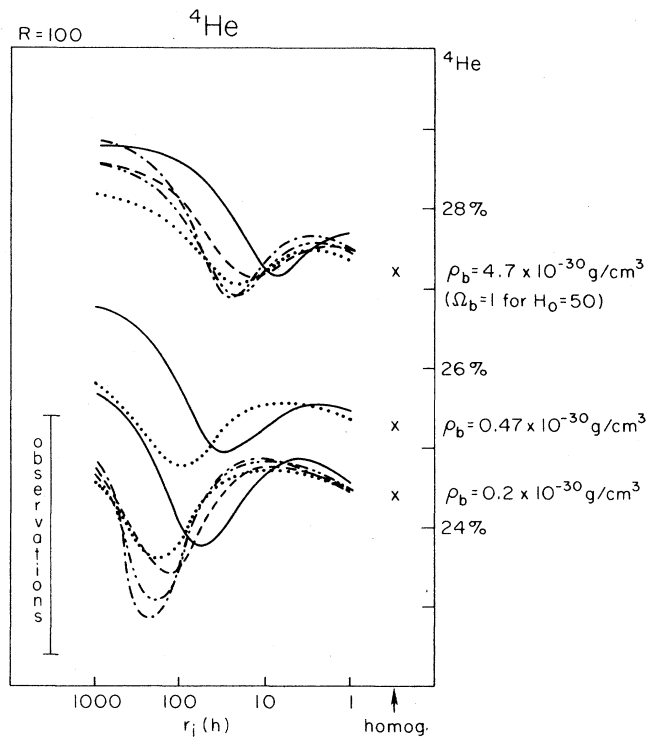


FIG. 2.  ${}^4\text{He}$  production (mass fraction) in our  $R=100$  runs. The results are plotted as a function of the distance-scale parameter  $r_1$  given in units of present light hours. This unit corresponds to about one meter at  $T=100 \text{ MeV}$  and to about 2.5 km at  $T=10^9 \text{ K}$ . As  $r_1$  becomes large, the results approach no-diffusion  $n_b/n_\gamma$ -inhomogeneity results. With small  $r_1$ , the results approach the homogeneous results ( $\times$ ) for the respective average baryon densities. Thus the curves form three groups according to the average baryon density used for the models. From top to bottom, we have  $\eta_{10}=70, \eta_{10}=7$ , and  $\eta_{10}=3$ . The vertical bar on the left denotes the observational range for primordial  ${}^4\text{He}$ . In Figs. 2–4, the different styles for the lines correspond to different geometries and high-density fractions:  $\cdots$ , plane,  $f_v=\frac{1}{4}$ ;  $-\cdots-$ , plane,  $f_v=\frac{1}{8}$ ;  $-\cdot-\cdot-$ , plane,  $f_v=\frac{1}{16}$ ;  $---$ , spherical (centrally condensed),  $f_v=\frac{1}{8}$ ;  $---$ , spherical (centrally condensed),  $f_v=\frac{1}{64}$ . It can be seen that the geometry has little effect on the results; the cylindrical geometries were intermediate between the plane and the spherical cases.

graphs show the transition from mere  $n_b/n_\gamma$  inhomogeneity with little diffusion at large distance scales, through strong  $n/p$  inhomogeneities created by neutron diffusion, towards the homogeneous results. For reference, the inhomogeneity from the quark-hadron phase transition has an estimated<sup>26</sup> upper limit  $r_i \lesssim 100$  h, and no lower limit is known.

How do these results answer the questions we asked in the Introduction? In short, answers to both of them seem to be negative. Let us go over them in detail.

*First question.* Are the observational constraints for  ${}^2\text{H}$ ,  ${}^4\text{He}$ , and  ${}^7\text{Li}$  satisfied in our  $\eta_{10}=70$  (closure density) runs?

${}^4\text{He}$ . There is only a narrow range of distance scales (within 5–50 h, depending on geometry) where neutron diffusion effects bring  ${}^4\text{He}$  below its homogeneous value, and then only very slightly. The lowest value in our runs with  $R=100, \eta_{10}=70$  was 26.9% (mass fraction), compared with the homogeneous result 27.2%. This is clearly above the observational range.

${}^2\text{H}$ . Baryon inhomogeneity can raise  ${}^2\text{H}$  production dramatically without any neutron diffusion effects. Our

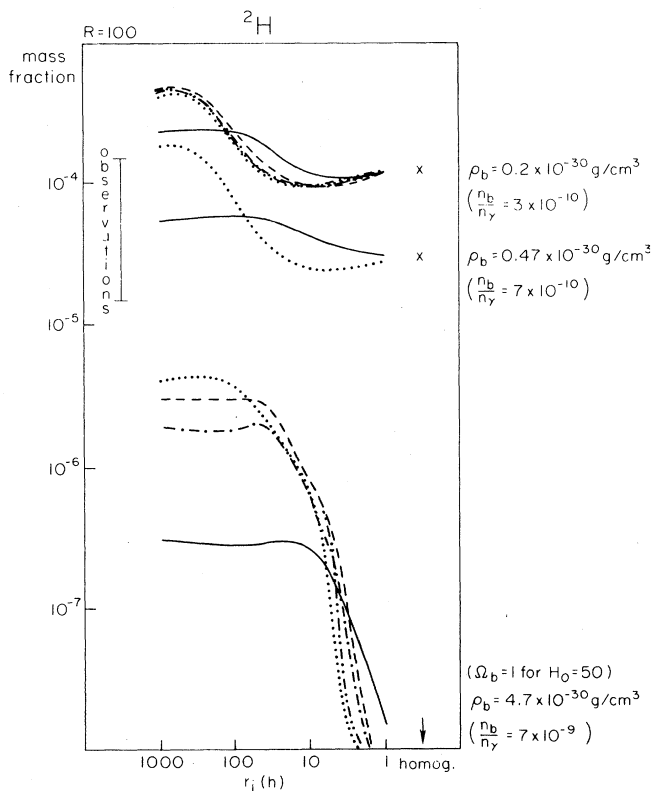


FIG. 3.  ${}^2\text{H}$  production in our  $R=100$  runs. The presentation is similar to that of  ${}^4\text{He}$  in Fig. 2. Now, however, the  $\eta_{10}=3$  group appears at the top and the  $\eta_{10}=70$  group at the bottom. The values are mass fractions. The homogeneous  $\eta_{10}=70$  value,  $1.5 \times 10^{-9}$ , did not fit into the graph. The smallest-scale ( $r_i < 10$  h) results for  ${}^2\text{H}$ , which fall very rapidly with decreasing  $r_i$ , did not satisfy our accuracy criterion ( $\pm 0.05$  in  $\log_{10} {}^2\text{H}$ ), being too sensitive to changes in time step and grid spacing.

results show that neutron diffusion does not bring any additional increase, in contrast with the simple-diffusion model. Instead, neutron diffusion begins to bring  ${}^2\text{H}$  down towards the homogeneous result. Thus, even if by adjusting the parameters we could raise  ${}^2\text{H}$  to the observational range for the largest  $r_i$ , the agreement would not extend to those  $r_i$  where neutron diffusion effects are shifting  ${}^4\text{He}$  and  ${}^7\text{Li}$  towards their observational range.

${}^7\text{Li}$ .  ${}^7\text{Li}$  was very high in all our  $R=100, \eta_{10}=70$  runs. There is a slight dip at the same values of  $r_i$  as for  ${}^4\text{He}$ , but not enough to bring  ${}^7\text{Li}$  even to the homogeneous  $\eta_{10}=70$  value.

*Second question.* In our  $\eta_{10}=3$  and  $\eta_{10}=7$  runs, is the agreement with observational values destroyed by  $R < 100$  inhomogeneity?

${}^2\text{H}$  and  ${}^4\text{He}$ . A baryon inhomogeneity without diffusion raises both  ${}^4\text{He}$  and  ${}^2\text{H}$  and thus destroys the agreement for any  $\eta$  if the inhomogeneity is strong enough. Our results show, however, that neutron diffusion effects bring both elements down, and thus the agreement is restored for  $r_i \lesssim 100$  h. Note that the effects have shifted towards larger distance scales than in the  $\eta_{10}=70$  case. That happens because (1) the lower proton density allows the neutrons to diffuse faster and (2) the nucleosynthesis happens later.

${}^7\text{Li}$ . The conclusions for  ${}^7\text{Li}$  depend on whether one believes in population I or population II stars as having

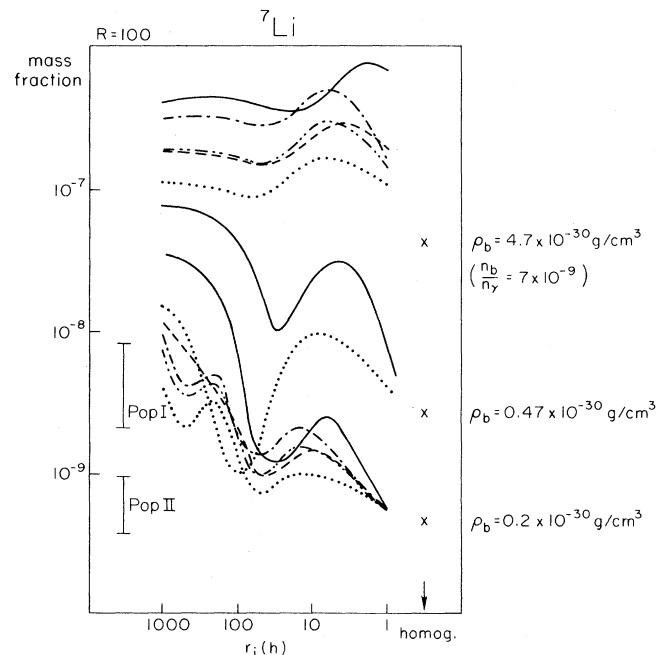


FIG. 4.  ${}^7\text{Li}$  production (mass fraction) in our  $R=100$  runs. The  $\eta_{10}=70$  group is at the top and the  $\eta_{10}=3$  group at the bottom. The closure density  $\eta_{10}=70$  curves are nowhere in agreement with observation. The  $\eta_{10}=7$  and  $\eta_{10}=3$  show a broad range ( $r_i \lesssim 100$ ) where these neutron-diffusion  $R=100$  calculations of  ${}^7\text{Li}$  are in agreement with observations if the homogeneous computations are.

the primordial  ${}^7\text{Li}$  mass fraction at their surfaces. The population II value, corresponding to the  ${}^7\text{Li}$  minimum in the homogeneous results, constrains nucleosynthesis very severely. However, our plane-symmetric  $R=100$ ,  $f_v = \frac{1}{4}$ ,  $\eta_{10}=3$  run kept  ${}^7\text{Li}$  within the population II constraints up to and including  $r_i=50$  h. Our  $\eta_{10}=7$  results show that if the average baryon density is away from the  ${}^7\text{Li}$  minimum, then baryon inhomogeneity with neutron diffusion can in some cases lower  ${}^7\text{Li}$  from the homogeneous value. Thus, we see no basis for claiming that  ${}^7\text{Li}$  would rule out strong baryon inhomogeneities. If  $r_i < 100$  h,  $R=100$  density contrast seems to be acceptable.

To save space, we do not show our results for the lower density contrasts, which were less interesting. They can be summarized by saying that they were qualitatively similar to the  $R=100$  results, but the effects were smaller. If one takes the homogeneous results as a reference point, in the  $f_v = \frac{1}{4}$  runs, going from  $R=100$  to  $R=10$  reduced the deviations to about  $\frac{1}{2}$  and going to  $R=6$  to about  $\frac{1}{4}$ . With  $f_v = \frac{1}{64}$  and  $R=10$ , the inhomogeneity effects were very small.

We also did some runs with a higher density contrast,  $R=1000$ , but it was difficult to obtain accurate results with our code in this case. For larger  $f_v$ , e.g.,  $f_v = \frac{1}{4}$ , the effect of a large density contrast begins to saturate above  $R=100$ , and results with  $R=1000$  were not very much different. Runs with a large  $R$  with a small  $f_v$  seemed to lead to the most dramatic results. We made an effort to obtain at least a few reliable numbers for this case. We chose  $R=1000$ ,  $f_v = \frac{1}{64}$  and from the less accurate runs chose those values of  $r_i$  where the diffusion seemed to have the strongest effect; we then redid these runs with a refined grid and shorter time step. The spherical case had the lowest  ${}^4\text{He}$  for  $r_i=5$  h. With 256 zones and 48 000 time steps, we finally obtained for this case  ${}^4\text{He} = 27.0\%$ ,  $\log_{10} {}^2\text{H} = -6.0$ ,  $\log_{10} {}^7\text{Li} = -6.1$ . For the planar case the lowest  ${}^4\text{He}$  was achieved with  $r_i=50$  h. We needed 512 zones and 48 000 time steps to get an accurate result:  ${}^4\text{He} = 26.6\%$ ,  $\log_{10} {}^2\text{H} = -5.5$ ,  $\log_{10} {}^7\text{Li} = -6.3$ . For the planar case the less accurate runs produced a sharp dip (as a function of  $r_i$ ) in  ${}^7\text{Li}$  at  $r_i=50$  h (our baseline run with 64 zones gave  $\log_{10} {}^7\text{Li} = -7.1$ ), raising false hopes of achieving low lithium, but with a finer zoning this effect was greatly reduced.

The parametrization  $f_v, R$  may not be the most appropriate one. If the high-density region already contains most of the baryons, large increases in  $R$  only lower the insignificant low-density value without appreciable change in the high-density value. We did a few runs with  $R=10^9$ , so that the low-density regions were extremely baryon poor. We did not expect a large change from the  $R=1000$  runs, but we noticed a curious effect. With the runs having the largest distance scales, where diffusion usually was not significant, we got very low  ${}^7\text{Li}$  values. These runs were perhaps rather inaccurate, but an examination of the details of these runs revealed what was going on: In the (extremely) low-density regions, nucleosynthesis never begins. Nucleosynthesis in the high-density regions consumes essentially all neutrons, dropping the

free-neutron density much below that of the low-density region. The low-density regions had a very low neutron density to begin with, of course, but these neutrons have remained free. Diffusion finally becomes important with these large distance scales. When nucleosynthesis has effectively ended in the high-density region, neutrons from the low-density region diffuse into it, destroying the  ${}^7\text{Be}$  there, thus leading to low final  ${}^7\text{Li}$ . Thus, we seem to have found the effect proposed by Malaney and Fowler<sup>11</sup> to solve the problem of  ${}^7\text{Li}$  overproduction, but in rather curious circumstances.

The charged nuclei diffuse much slower than neutrons. Can their diffusion be ignored? We have included the diffusion of protons in our model. To answer the question, we did a few runs ( $\eta_{10}=70, R=100, f_v = \frac{1}{64}, r_i=1-100$ , spherical) with proton diffusion disabled. There was no appreciable change in other abundances except for  ${}^2\text{H}$ . Without proton diffusion we got higher  ${}^2\text{H}$  production.  ${}^2\text{H}$  actually then had a shallow peak (as a function of  $r_i$ ) at  $r_i=20$ , where it exceeded the with-proton-diffusion value by  $\frac{1}{3}$ . The relative difference grew with smaller  $r_i$  (as the  ${}^2\text{H}$  production went down), and was a factor of 2 at  $r_i=1$ .

#### IV. CONCLUSION

We arrived at a negative answer to both questions we asked in the Introduction. With a critical baryon density,  $\eta_{10}=70$ , all three abundances,  ${}^4\text{He}$ ,  ${}^2\text{He}$ , and  ${}^7\text{Li}$ , remain in significant disagreement with observations, even with a density contrast as high as  $R=100$ . If the density contrast is smaller, the results will be even closer to the homogeneous results and substantially in disagreement with observations.

There remains, of course, the possibility that an agreement could be found with an even more extreme inhomogeneity. Our  $R=100$  runs did have indications of change toward the right direction for all three abundances; a baryon inhomogeneity raises  ${}^2\text{H}$ , and neutron diffusion effects caused a dip in  ${}^4\text{He}$  and  ${}^7\text{Li}$  for intermediate distance scales. We did some runs with higher values of  $R$  and saw that those effects did become stronger. Because it became very expensive to obtain accurate results for very large  $R$ , we did not attempt an extensive survey of those. For very large  $R$  with  $f_v \ll 1$  and  $f_v R \gg 1$ , a simultaneous agreement might be found with some parameter values for a narrow range in  $r_i$ . In addition to requiring fine-tuning the distance scale, such a result would face the difficulty of explaining where such inhomogeneities could come from. In an earlier paper<sup>7</sup> we presented a scenario for the quark-hadron phase transition, where the inhomogeneity would appear as sharp spikes so that the density contrast indeed might be very large. But in this scenario the total amount of baryons in those spikes was small, so that  $f_v R \ll 1$ , leading to negligible effect on nucleosynthesis.

Nucleosynthesis results cannot be used to rule out strong small-scale,  $r_i < 100$  h, prenucleosynthesis inhomogeneities in the baryon density. For larger scales, the old baryon inhomogeneity results without diffusion apply,

and very strong inhomogeneities are ruled out by overproduction of  ${}^7\text{Li}$  and either  ${}^4\text{He}$  or  ${}^2\text{H}$ , depending on average density.

Nucleosynthesis cannot be used to constrain the baryon density contrast across a quark-hadron phase interface for at least three reasons. (1) It is not clear how the resulting inhomogeneity after the phase transition is related to this density contrast during the phase transition. (2) The distance scale of the bubble/droplet structure during the phase transition has not been determined; it could be too small to affect nucleosynthesis (our results for the smallest  $r_i$  approached the homogeneous results). (3) The results presented here show that the predicted baryon inhomogeneity leaves no strong signature in the final nuclear abundances.

If one wished to use nucleosynthesis to tell us something about the parameters of the quark-hadron phase transition, we can only offer the following: To get significant effects on nucleosynthesis—if that is desirable, perhaps in the pursuit of the critical baryon density—the distance scale has to be fairly large, close to Hogan's upper limit.<sup>26</sup> One can then study the quark-hadron phase transition with this assumption. With a large distance scale it becomes difficult to see how the baryon-density contrast developing at the phase interface could extend itself to the interiors of the regions. Thus, we would just expect relatively thin layers of high baryon density. After the hadron bubbles have touched, the structure of the region remaining in the quark phase would be too large scale for surface tension to pull the baryons into spherical droplets.<sup>1</sup> Thus, the remaining structure and the shape of any resulting baryon inhomogeneity would not be spherical blobs, but rather sheets and filaments. A large-scale structure also would imply deep supercooling before the transition, leading to entropy generation, shock waves in the beginning of the transition, and an energy density inhomogeneity after the transition.<sup>26–29</sup>

*Note added in proof.* The decrease of  ${}^4\text{He}$  by 0.002–0.003 due to corrections to the weak rates calculated by Dicus *et al.*<sup>30</sup> has not been included in our results.

Fowler<sup>31</sup> has called to our attention the reaction  ${}^7\text{Li}(n,\gamma){}^8\text{Li}$ , which in standard nucleosynthesis is insignificant but could affect lithium abundance in late-time neutron-rich conditions of nonstandard nucleosynthesis. We have looked at the effect of this reaction by adding it as a sink and using the theoretical rate given by Malandy and Fowler.<sup>9</sup> In our computations the final averaged  ${}^7\text{Li}$  is affected for small  $\eta$  and large  $r_i$  only and even then by not more than about 1% decrease.

In the high-density models most of the final  ${}^7\text{Li}$  is in the form of  ${}^7\text{Be}$  during the end stages of nucleosynthesis. Thus, the main effect of late-time neutrons is through  ${}^7\text{Be}(n,\alpha){}^4\text{He}$  and  ${}^7\text{Be}(n,p){}^7\text{Li}$ , of which the latter has the larger rate [ ${}^7\text{Li}$  is then consumed by several reactions, e.g.  ${}^7\text{Li}(p,\alpha){}^4\text{He}$  and  ${}^7\text{Li}(d,n\alpha){}^4\text{He}$ ]. This can indeed cause significant reduction in the final  ${}^7\text{Li}$  for the intermediate-distance scales, as discovered by Malaney and Fowler.<sup>11</sup> As can be seen from Fig. 4, the effect is especially strong for the  $\rho_b = 0.47 \times 10^{-30}$  g/cm<sup>3</sup> case. For a critical baryon density, the effect is weaker because fewer neutrons survive until the late stages. Mathews, Fuller, Alcock, and Kajino<sup>32</sup> have done a calculation where by using an extremely high density contrast (over 20 000) they have found a length scale (their  $l = 30$  m corresponds to our  $r_i = 10$  h), where the predicted abundances (except  ${}^7\text{Li}$ ) for a critical baryon density can be brought to agreement with observations. To us, a density contrast this high appears unrealistic.

#### ACKNOWLEDGMENTS

We thank Professor K. Olive for bringing the question of  ${}^7\text{Li}$  consistency to our attention, and Dr. James R. Wilson for his enthusiasm for this project and for important technical suggestions. This work was supported in part by NSF Grants Nos. PHY84-04931, PHY88-06567, PHY84-51732, and PHY87-06315. The computations were performed at the National Center for Supercomputing Applications, University of Illinois at Urbana-Champaign.

<sup>1</sup>E. Witten, Phys. Rev. D **30**, 272 (1984).

<sup>2</sup>J. H. Applegate and C. J. Hogan, Phys. Rev. D **31**, 3037 (1985).

<sup>3</sup>J. H. Applegate, C. J. Hogan, and R. J. Scherrer, Phys. Rev. D **35**, 1151 (1987).

<sup>4</sup>C. Alcock, G. M. Fuller, and G. J. Mathews, Astrophys. J. **320**, 439 (1987).

<sup>5</sup>J. H. Applegate, C. J. Hogan, and R. J. Scherrer, Astrophys. J. **329**, 572 (1988).

<sup>6</sup>G. M. Fuller, G. J. Mathews, and C. R. Alcock, Phys. Rev. D **37**, 1380 (1988).

<sup>7</sup>H. Kurki-Suonio, Phys. Rev. D **37**, 2104 (1988).

<sup>8</sup>R. A. Matzner, T. Rothman, J. M. Centrella, and J. R. Wilson, in *Origin and Distribution of the Elements*, edited by G. J. Mathews (World Scientific, Singapore, 1988).

<sup>9</sup>R. A. Malaney and W. A. Fowler, in *Origin and Distribution of the Elements* (Ref 8).

<sup>10</sup>H. Kurki-Suonio, R. A. Matzner, J. M. Centrella, T. Roth-

man, and J. R. Wilson, Phys. Rev. D **38**, 1091 (1988).

<sup>11</sup>R. A. Malaney and W. A. Fowler, Astrophys. J. **333**, 14 (1988).

<sup>12</sup>N. Terasawa and K. Sato, University of Tokyo Report No. UTAP77, 1988 (unpublished).

<sup>13</sup>J. Yang, M. S. Turner, G. Steigman, D. N. Schramm, and K. A. Olive, Astrophys. J. **281**, 493 (1984).

<sup>14</sup>A. M. Boesgaard and G. Steigman, Annu. Rev. Astron. Astrophys. **23**, 319 (1985).

<sup>15</sup>H. Reeves, in *Frontiers and Borderlines in Many Particle Physics*, proceedings of the Enrico Fermi International Summer School of Physics, Varenna, Italy, 1987, edited by R. A. Broglia and J. R. Schrieffer (North-Holland, Amsterdam, in press); also symposium talk in Bologna, as reported by New Scientist, 30 June (1988), p. 46; K. Olive, Nature (London) **330**, 700 (1988).

<sup>16</sup>J. Centrella and J. R. Wilson, Astrophys. J. **273**, 428 (1983).

- <sup>17</sup>J. Centrella and J. R. Wilson, *Astrophys. J. Suppl. Series* **54**, 229 (1984).
- <sup>18</sup>J. Centrella, R. A. Matzner, T. Rothman, and J. R. Wilson, *Nucl. Phys.* **B266**, 171 (1986).
- <sup>19</sup>H. Kurki-Suonio, in *Frontiers in Numerical Relativity*, edited by C. Evans, S. Finn, and D. Hobill (Cambridge University Press, Cambridge, England, 1988).
- <sup>20</sup>S. Gottlieb, W. Liu, D. Toussaint, R. L. Renken, and R. L. Sugar, *Phys. Rev. Lett.* **59**, 2247 (1987).
- <sup>21</sup>J. I. Kapusta and K. A. Olive, *Phys. Lett. B* **209**, 295 (1988).
- <sup>22</sup>W. A. Fowler, G. R. Caughlan, and B. A. Zimmermann, *Annu. Rev. Astron. Astrophys.* **5**, 525 (1967).
- <sup>23</sup>W. A. Fowler, G. R. Caughlan, and B. A. Zimmermann, *Annu. Rev. Astron. Astrophys.* **13**, 69 (1975).
- <sup>24</sup>M. J. Harris, W. A. Fowler, G. R. Caughlan, and B. A. Zimmermann, *Annu. Rev. Astron. Astrophys.* **21**, 165 (1983).
- <sup>25</sup>This is the 1988 Particle Data Group value [*Phys. Lett. B* **204**, 1 (1988)].
- <sup>26</sup>C. J. Hogan, *Phys. Lett.* **133B**, 172 (1983).
- <sup>27</sup>M. Gyulassy, K. Kajantie, H. Kurki-Suonio, and L. McLerran, *Nucl. Phys.* **B237**, 477 (1984).
- <sup>28</sup>H. Kurki-Suonio, *Nucl. Phys.* **B255**, 231 (1985).
- <sup>29</sup>K. Kajantie and H. Kurki-Suonio, *Phys. Rev. D* **34**, 1719 (1986).
- <sup>30</sup>D. A. Dicus, E. W. Kolb, A. M. Gleeson, E. C. G. Sudarshan, V. L. Teplitz, and M. S. Turner, *Phys. Rev. D* **26**, 2694 (1982).
- <sup>31</sup>W. A. Fowler (private communication).
- <sup>32</sup>G. J. Mathews, G. M. Fuller, C. R. Alcock, and T. Kajino, in *Proceedings of the 8th Moriond Astrophysics Meeting on Dark Matter, Les Arcs, France, 1988* (unpublished).